Preprint typeset in JHEP style - HYPER VERSION

Feynman Rules for the Rational Part of the QCD 1-loop amplitudes

P. Draggiotis

Departamento de Física Teórica y del Cosmos y CAFPE Universidad de Granada, E-18071 Granada, Spain.
E-mail: pdrangiotis@ugr.es

M.V. Garzelli

Departamento de Física Teórica y del Cosmos y CAFPE Universidad de Granada, E-18071 Granada, Spain and INFN Milano, I-20133 Milano, Italy.
E-mail: garzelli@to.infn.it

C.G. Papadopoulos

Institute of Nuclear Physics, NCSR Demokritos, 15310 Athens, Greece.
E-mail: costas.papadopoulos@cern.ch

R. Pittau

Departamento de Física Teórica y del Cosmos y CAFPE Universidad de Granada, E-18071 Granada, Spain.
E-mail: pittau@ugr.es

Abstract: We compute the complete set of Feynman Rules producing the Rational Terms of kind R_2 needed to perform any QCD 1-loop calculation. We also explicitly check that in order to account for the entire R_2 contribution, even in case of processes with more than four external legs, only up to four-point vertices are needed. Our results are expressed both in the 't Hooft Veltman regularization scheme and in the Four Dimensional Helicity scheme, using explicit color configurations as well as the color connection language.

Keywords: NLO, radiative corrections.

Contents

1. Introduction

In the last few years, the problem of computing one-loop amplitudes efficiently has been attacked by several groups. Standard techniques, such as the Passarino-Veltman [1] tensor reduction and its many variances [2]-[4], have been used for many years, and have produced a great deal of useful results [5]. Nowadays new developments, in which the amplitude is directly reconstructed are widely used. Such approaches rely on the fact that the basis of one-loop scalar integrals is known in terms of Boxes, Triangles, Bubbles and (in massive theories) Tadpoles, so that any one-loop amplitude $\mathcal{M}$ can then be written as:

$$\mathcal{M} = \sum_i d_i \text{ Box}_i + \sum_i c_i \text{ Triangle}_i + \sum_i b_i \text{ Bubble}_i + \sum_i a_i \text{ Tadpole}_i + \mathrm{R}\,, \qquad (1.1)$$

where d_i, c_i, b_i and a_i are the coefficients to be determined and R is a remaining piece, called Rational Term (RT). The first attempt in this direction was the Unitarity approach [6], by Bern, Dixon and Kososwer, in which two-particle cuts are performed on the one-loop amplitude (or, equivalently, two tree-level amplitudes are glued) in order to get information on the coefficients in eq. 1.1. The method produced many useful – mainly analytical – results, especially for massless theories [7], but a systematic way to determine all the coefficients of eq. 1.1 was missing.

Later it was shown by Britto Cachazo and Feng [8] that the d_i coefficients can be easily separated from the rest and computed by introducing quadruple cuts in which the loop integration momentum is completely frozen by four on-shell conditions. It was then possible to perform a full reconstruction of the amplitude for theories with only boxes,

such as N = 4 super-Yang-Mills. However, a systematic procedure to get all the other coefficients was still missing.

Recently the problem of determining in a systematic way the coefficients d_i, c_i, b_i and a_i was completely solved by the OPP method of refs. [9] and [10]. Within this method, eq. 1.1 is substituted by its unintegrated counterpart, at the price of introducing the so called spurious terms, defined by the property of vanishing upon integration over the loop momentum q. In practice, since the functional form in q of the spurious terms is universal, one has to find, besides d_i, c_i, b_i, and a_i, an additional set of coefficients. The OPP method allows to find all those coefficients by computing the unintegrated amplitude at different values of q for which 4, 3, 2 and 1 propagators vanish. At each stage, the coefficient that have been already computed are numerically subtracted from the original amplitude, so that, by using such an OPP subtraction, it is possible to disentangle all the coefficients in a systematic way. The OPP approach was inspired by the unitarity method and the tensor reduction at the integrand level [11].

More recently the OPP subtraction method was used by the authors of [12] together with the Unitarity approach, giving rise to the so called generalized Unitarity techniques, that, nowadays, include both semi-analytical [13] and fully numerical versions [14]-[15]. Nevertheless, in practice, only the so called cut-constructible part of the amplitude, namely that one proportional to the one-loop scalar functions, can be easily obtained. The remaining Rational Terms R [16]-[17] require some additional work. For instance, in [14] the Rational part is obtained by explicitly computing the amplitude at different integer values of the space-time dimensions (n). Other possibilities are to get them through n-dimensional cuts [18] or with the help of recursion relations [19].

On the other hand, in the OPP method, two classes of terms contributing to R naturally arise [20]. The first class, called R_1, can be derived straightforwardly within the same framework used to determine all other coefficients, while the second class, called R_2, is coming from the $(n-4)$-dimensional part of the amplitude and can be obtained by computing, once for all, tree-level like Feynman Rules for the theory under study. Moreover, it is worthwhile to mention that only the full $\mathrm{R} = \mathrm{R}_1 + \mathrm{R}_2$ constitutes a physical gauge-invariant quantity in dimensional regularization. On the other hand, R_1 can be directly read out from the analytic expressions of the cut-constructible part of the amplitude, irrespectively of the method used to derive it.

In this paper, we explicitly compute the entire set of Feynman Rules producing R_2 needed in any (massive or massless) QCD 1-loop calculation. We perform our calculation in the $\xi = 1$ 't Hooft-Feynman gauge. As a consequence, also the δZ couterterms [2] needed to build renormalized scattering amplitudes should be computed in the $\xi = 1$ gauge.

In the next section we briefly recall the origin of R_2 and give a detailed computational example. In section 3, we list our results and present numerical comparisons with known amplitudes. In section 4 we draw our conclusions and, in three appendices, we collect diagrams and formulae used for the calculation as well as our results expressed in the color connection language.

2. The origin of R_2

Before carrying out our program, we spend a few more words on the origin of R_2, that is also necessary for setting up the framework of our calculation.

Our starting point is the general expression for the *integrand* of a generic m-point one-loop (sub-)amplitude

$$\bar{A}(\bar{q}) = \frac{\bar{N}(\bar{q})}{\bar{D}_0 \bar{D}_1 \cdots \bar{D}_{m-1}}, \quad \bar{D}_i = (\bar{q} + p_i)^2 - m_i^2, \tag{2.1}$$

where $\bar{q}$ is the integration momentum. In the previous equation, dimensional regularization is assumed, so that we use a bar to denote objects living in $n = 4 + \epsilon$ dimensions and a tilde to represent ϵ-dimensional quantities. Notice that, when a n-dimensional index is contracted with a 4-dimensional (observable) vector v_μ, the 4-dimensional part is automatically selected. For example

$$\bar{q} \cdot v \equiv (q + \tilde{q}) \cdot v = q \cdot v \quad \text{and} \quad \bar{\not{v}} \equiv \bar{\gamma}_{\bar{\mu}} v^\mu = \not{v}. \tag{2.2}$$

An important consequence is

$$\bar{q}^2 = q^2 + \tilde{q}^2. \tag{2.3}$$

The numerator function $\bar{N}(\bar{q})$ can be further split into a 4-dimensional plus an ϵ-dimensional part

$$\bar{N}(\bar{q}) = N(q) + \tilde{N}(\tilde{q}^2, q, \epsilon). \tag{2.4}$$

$N(q)$ lives in 4-dimensions while $\tilde{N}(\tilde{q}^2, q, \epsilon)$, once integrated, gives rise to the RTs of kind R_2, defined as

$$R_2 \equiv \frac{1}{(2\pi)^4} \int d^n \bar{q} \frac{\tilde{N}(\tilde{q}^2, q, \epsilon)}{\bar{D}_0 \bar{D}_1 \cdots \bar{D}_{m-1}}. \tag{2.5}$$

To investigate the explicit form of $\tilde{N}(\tilde{q}^2, q, \epsilon)$ it is important to understand better the separation in eq. 2.4. From a given *integrand* $\bar{A}(\bar{q})$ this is obtained by splitting, in the numerator function, the n-dimensional integration momentum $\bar{q}$, the n-dimensional gamma matrices $\bar{\gamma}_{\bar{\mu}}$ and the n-dimensional metric tensor $\bar{g}^{\bar{\mu}\bar{\nu}}$ into a 4-dimensional component plus remaining pieces:

$$\begin{aligned} \bar{q} &= q + \tilde{q}, \\ \bar{\gamma}_{\bar{\mu}} &= \gamma_\mu + \tilde{\gamma}_{\tilde{\mu}}, \\ \bar{g}^{\bar{\mu}\bar{\nu}} &= g^{\mu\nu} + \tilde{g}^{\tilde{\mu}\tilde{\nu}}. \end{aligned} \tag{2.6}$$

A practical way to determine R_2 is then computing, once for all and with the help of eq. 2.6, tree-level like Feynman Rules by calculating the R_2 part coming from one-particle irreducible amplitudes up to four external legs. The fact that four external legs are enough is guaranteed by the ultraviolet nature of the RTs, proven in [16]. Through eq. 2.5 a set

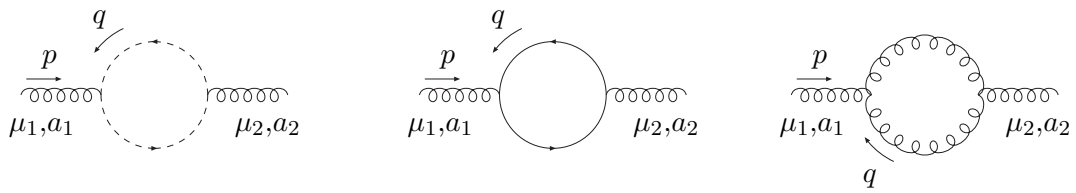

Figure 1: *Diagrams contributing to the gluon self-energy.*

of basic integrals with up to 4 denominators is generated, containing powers of $\tilde{q}$ and ϵ in the numerator. A list that exhausts all possibilities in the $\xi = 1$ 't Hooft-Feynman gauge is presented in appendix A. Notice that, according to the chosen regularization scheme, results may differ. In eq. 2.5 we use the 't Hooft-Veltman (HV) scheme, while in the Four Dimensional Helicity scheme (FDH), any explicit ϵ dependence in the numerator function is discarded before integration. Therefore

$$\mathrm{R}_2\Big|_{FDH} = \frac{1}{(2\pi)^4}\int d^n\,\bar{q}\frac{\tilde{N}(\tilde{q}^2,q,\epsilon=0)}{\bar{D}_0\bar{D}_1\cdots\bar{D}_{m-1}}\,. \tag{2.7}$$

As an explicit and simple example of the described procedure, we detail the calculation of R_2 coming from the gluon self-energy. The contributing diagrams [1] are drawn in fig. 1.

As for the ghost loop with 2 external gluons, we can write the numerator as

$$\bar{N}(\bar{q}) = \frac{g^2}{(2\pi)^4} f^{a_1bc}\, f^{a_2cb}\,(p+\bar{q})^{\mu_1}\,\bar{q}^{\mu_2}\,. \tag{2.8}$$

Since μ_1 and μ_2 are external Lorentz indices, that are eventually contracted with 4-dimensional external currents, their ϵ-dimensional component is killed due to eq. 2.2. Therefore, $\mathrm{R}_2 = 0$ for this diagram, being $\tilde{N}(\tilde{q}^2,q,\epsilon) = 0$. With this same reasoning, one easily shows that ghost loops never contribute to R_2, even with 3 or 4 external gluons.

The contribution due to N_f quark loops is given by the second diagram of fig. 1, whose numerator reads

$$\bar{N}(\bar{q}) \,=\, -\frac{g^2}{(2\pi)^4}N_f\frac{\delta_{a_1a_2}}{2}\,Tr[\gamma^{\mu_1}(\not{\bar{q}}+m_q)\gamma^{\mu_2}(\not{\bar{q}}+\not{p}+m_q)]\,, \tag{2.9}$$

where the external indices μ_1 and μ_2 have been directly taken in 4 dimensions. By anti-commuting γ^{μ_2} and $\not{\bar{q}}$ and using the fact that, due to Lorentz invariance, odd powers of $\tilde{q}$ do no contribute, one immediately arrives at the result

$$\tilde{N}(\tilde{q}^2) = \frac{g^2}{8\pi^4}\,N_f\,\delta_{a_1a_2}\,g_{\mu_1\mu_2}\tilde{q}^2\,. \tag{2.10}$$

Eq. 2.10, integrated with the help of the first one of eqs. A.1, gives the term proportional to N_f in the 2-point effective vertex of fig. 2.

[1] Our conventions and notations are listed in Appendix B.

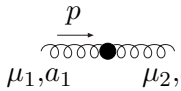

$$= \frac{ig^2 N_{col}}{48\pi^2}\,\delta_{a_1a_2}\Big[\,\frac{p^2}{2}g_{\mu_1\mu_2} + \lambda_{HV}\left(g_{\mu_1\mu_2}p^2 - p_{\mu_1}p_{\mu_2}\right) + \frac{N_f}{N_{col}}\left(p^2 - 6\,m_q^2\right)g_{\mu_1\mu_2}\Big]$$

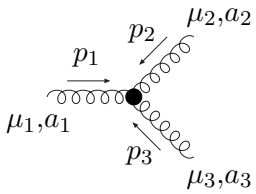

$$= -\frac{g^3 N_{col}}{48\pi^2}\left(\frac{7}{4} + \lambda_{HV} + 2\frac{N_f}{N_{col}}\right) f^{a_1a_2a_3}\,V_{\mu_1\mu_2\mu_3}(p_1,p_2,p_3)$$

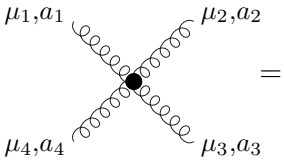

$$= -\frac{ig^4 N_{col}}{96\pi^2}\sum_{P(234)}\Bigg\{\Big[\,\frac{\delta_{a_1a_2}\delta_{a_3a_4} + \delta_{a_1a_3}\delta_{a_4a_2} + \delta_{a_1a_4}\delta_{a_2a_3}}{N_{col}} + 4\,Tr(t^{a_1}t^{a_3}t^{a_2}t^{a_4} + t^{a_1}t^{a_4}t^{a_2}t^{a_3})\,(3+\lambda_{HV}) - Tr(\{t^{a_1}t^{a_2}\}\{t^{a_3}t^{a_4}\})\,(5+2\lambda_{HV})\Big]\,g_{\mu_1\mu_2}g_{\mu_3\mu_4} + 12\frac{N_f}{N_{col}}Tr(t^{a_1}t^{a_2}t^{a_3}t^{a_4})\left(\frac{5}{3}g_{\mu_1\mu_3}g_{\mu_2\mu_4} - g_{\mu_1\mu_2}g_{\mu_3\mu_4} - g_{\mu_2\mu_3}g_{\mu_1\mu_4}\right)\Bigg\}$$

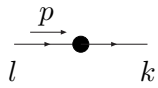

$$= \frac{ig^2}{16\pi^2}\frac{N_{col}^2 - 1}{2N_{col}}\delta_{kl}(-\not{p} + 2m_q)\,\lambda_{HV}$$

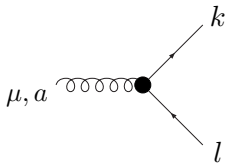

$$= \frac{ig^3}{16\pi^2}\frac{N_{col}^2 - 1}{2N_{col}}\,t^a_{kl}\gamma_\mu\,(1+\lambda_{HV})$$

Figure 2: *Effective vertices contributing to* R_2 *in pure QCD.* $\sum_{P(234)}$ *stands for a summation over the six permutations of the indices 2, 3 and 4, and* $\{t^{a_i}t^{a_j}\} \equiv t^{a_i}t^{a_j} + t^{a_j}t^{a_i}$. $\lambda_{HV} = 1$ *in the HV scheme and* $\lambda_{HV} = 0$ *in the FDH scheme.* N_{col} *is the number of colors and* N_f *is the number of fermions running in the quark loop.*

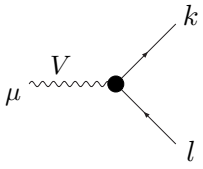

$$= -\frac{g^2}{16\pi^2}\frac{N_{col}^2-1}{2N_{col}}\,\delta_{kl}\gamma_\mu\,(v+a\gamma_5)\,(1+\lambda_{HV})$$

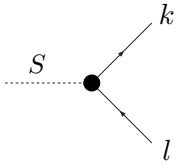

$$= -\frac{g^2}{8\pi^2}\frac{N_{col}^2-1}{2N_{col}}\,\delta_{kl}\,(c+d\gamma_5)\,(1+\lambda_{HV})$$

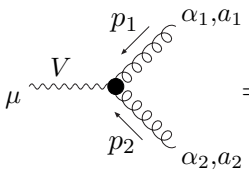

$$= -a\,\frac{ig^2}{12\pi^2}\,\delta_{a_1a_2}\epsilon_{\mu\alpha_1\alpha_2\beta}\,(p_1-p_2)^\beta$$

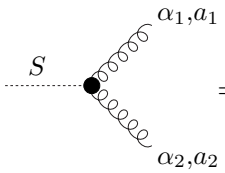

$$= c\,\frac{g^2}{8\pi^2}\,\delta_{a_1a_2}g_{\alpha_1\alpha_2}\,m_q$$

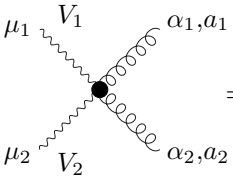

$$= -\frac{ig^2}{24\pi^2}\,\delta_{a_1a_2}(v_1v_2+a_1a_2)\,(g_{\mu_1\mu_2}g_{\alpha_1\alpha_2}+g_{\mu_1\alpha_1}g_{\mu_2\alpha_2}+g_{\mu_1\alpha_2}g_{\mu_2\alpha_1})$$

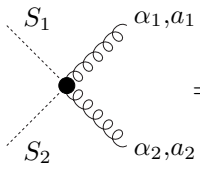

$$= \frac{ig^2}{8\pi^2}\,\delta_{a_1a_2}\,(c_1c_2-d_1d_2)\,g_{\alpha_1\alpha_2}$$

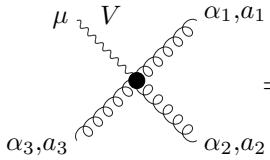

$$= -\frac{g^3}{24\pi^2}\,\{v\,Tr(t^{a_1}\{t^{a_2}t^{a_3}\})(g_{\mu\alpha_1}g_{\alpha_2\alpha_3}+g_{\mu\alpha_2}g_{\alpha_1\alpha_3}+g_{\mu\alpha_3}g_{\alpha_1\alpha_2})$$
$$-i9a\,\left[Tr(t^{a_1}t^{a_2}t^{a_3})-Tr(t^{a_1}t^{a_3}t^{a_2})\right]\,\epsilon_{\mu\alpha_1\alpha_2\alpha_3}\}$$

Figure 3: *Effective vertices contributing to* R_2 *in mixed QCD.* $\lambda_{HV}=1$ *in the HV scheme and* $\lambda_{HV}=0$ *in the FDH scheme. In the case of neutral external vectors or scalars, the formulae should be read as the contribution given by one quark loop. In the case of charged external particles, they refer instead to the contribution of one quark family.*

Finally, the numerator function of the diagram with a gluonic loop reads

$$\bar{N}(\bar{q}) = -\frac{g^2}{2(2\pi)^4} f^{a_1 bc} f^{a_2 cb} V_{\mu_1 \bar{\beta}\bar{\gamma}}(p, -\bar{q}-p, \bar{q}) V_{\mu_2}{}^{\bar{\gamma}\bar{\beta}}(-p, -\bar{q}, \bar{q}+p)\,, \tag{2.11}$$

with V given in eq. B.1. The contraction of the two V tensors gives terms containing

$$\bar{q}^2 = q^2 + \tilde{q}^2\,, \quad \text{and} \quad \bar{g}_{\bar{\alpha}\bar{\beta}}\,\bar{g}^{\bar{\alpha}\bar{\beta}} = 4 + \epsilon\,, \tag{2.12}$$

from which one obtains

$$\tilde{N}(\tilde{q}^2, q, \epsilon) = -\frac{g^2}{2(2\pi)^4} f^{a_1 bc} f^{a_2 cb} \Big[\, 2 g_{\mu_1\mu_2}\tilde{q}^2 + 4\epsilon q_{\mu_1} q_{\mu_2} + 2\epsilon q_{\mu_1} p_{\mu_2} + 2\epsilon p_{\mu_1} q_{\mu_2} + \epsilon p_{\mu_1} p_{\mu_2} \,\Big]\,. \tag{2.13}$$

Performing the integration, gives the expression written in the first line of fig. 2, where the contribution proportional to λ_{HV} is generated by the ϵ dependence of eq. 2.13.

The complete set of effective vertices obtained with the described technique is presented in the next section.

3. Results

As already explained, 1-loop irreducible Feynman diagrams up to 4 external legs are sufficient to compute R_2 for any amplitude with any number of external legs. Each contributing diagram has been calculated analytically by using the Feynman rules listed in appendix B, which also contains the list of the relevant graphs. Different contributions have then been summed and reorganized to identify the effective R_2 vertices listed in figs. 2 and 3, which represent the main result of this work and that allow to determine R_2 needed in the computation of the NLO QCD corrections to any process in the Standard Model.

In fig. 2 we collect the "pure" QCD effective vertices, namely all vertices generated by QCD corrections to processes with external QCD particles. The complete set of contributing diagrams is given in fig. 5. In fig. 3 we list, instead, the "mixed" QCD vertices generated by QCD corrections to processes containing at least one external electroweak particle. In this paper, this last class is parametrized by introducing generic couplings of a (pseudo)-vector and of a (pseudo)-scalar with a quark line, as in the last two vertices of fig. 4. The non vanishing diagrams contributing to R_2 are listed in fig. 6.

In all figures, N_{col} is the number of colours, N_f is the number of fermions running in the quark loop and λ_{HV} is a parameter allowing to read our formulae in two different regularization schemes: $\lambda_{HV} = 1$ corresponds to the HV scheme of eq. 2.5 while $\lambda_{HV} = 0$ in the FDH scheme defined in eq. 2.7.

Notice that the whole structure of the three-gluon effective vertex is always proportional to the tree-level, while the four-gluon effective vertex is more complicated.

Notice also that, when a completely antisymmetric ϵ tensor occur in the formulae of the mixed QCD vertices, it always multiplies the axial coupling a. Therefore, summing over all quark loops gives zero in the Standard Model, due to the anomaly cancellation. Such terms can then be taken to be zero from the very beginning.

In figs. 2 and 3 the effective vertices are given in terms of traces of color matrices and structure constants. The same result in terms of color connections is presented in appendix C.

Just as a showcase of our ability to reproduce the rational terms R_2 correctly for higher multiplicity of external legs, we have computed the 1-loop six gluon amplitude using an extension [21] of `HELAC-PHEGAS` [22], `HELAC-1loop`, that includes virtual corrections through an interface with `CutTools` [10].

The comparison against the results of ref. [23] is given in table 1, that refers to one color configuration only and to the following phase space point:

$$\begin{aligned}
p_1 &= (-3.000000000000000, 1.837117307087384, -2.121320343559642, 1.060660171779821)\\
p_2 &= (-3.000000000000000, -1.837117307087384, 2.121320343559642, -1.060660171779821)\\
p_3 &= (2.000000000000000, 0.000000000000000, -2.000000000000000, 0.000000000000000)\\
p_4 &= (0.857142857142857, 0.000000000000000, 0.315789473684211, 0.796850604480708)\\
p_5 &= (1.000000000000000, 0.866025403784439, 0.184210526315789, 0.464829519280413)\\
p_6 &= (2.142857142857143, -0.866025403784439, 1.500000000000000, -1.261680123761121) \qquad (3.1)
\end{aligned}$$

We find an excellent agreement among the results when including the R_2 contribution. Finally, we mention that, always with the help of `HELAC-1loop`, we successfully compared our predictions for six-quark 1-loop amplitudes (with three different flavours) with the results produced by the GOLEM group [4]. In addition, for all sub-processes included in the 2007 Les Houches wish list [24], we explicitly checked that the validity of the Ward Identity for a single on-shell external gluon (when present) is preserved by the sum $R_1 + R_2$.

4. Conclusions

We have derived the tree-level Feynman rules needed to compute the Rational Terms R_2 in QCD, both using explicit color configurations and in the color connection language. We listed all effective vertices generated by QCD corrections to processes with external QCD particles and all possible mixed QCD effective vertices generated by QCD corrections to processes with at least one external EW particle. The inclusion of the derived vertices in an actual calculation gives numerical agreement with known expressions for processes up to 6 external legs. So we have explicitly checked that 1,2,3 and 4-point vertices are enough to solve the problem for an arbitrary number of external legs. In addition, all relevant integrals needed to compute R_2 in the $\xi = 1$ 't Hooft-Feynman gauge have been explicitly listed. The next obvious step is the determination of the Feynman Rules needed in the complete Standard Model. We leave this for a future publication.

Acknowledgments

We would like to thank Giovanni Ossola and Thomas Binoth for many useful discussions. R.P. acknowledges the financial support of the ToK Program "ALGOTOOLS" (MTKD-CD-2004-014319). P.D.'s, C.G.P.'s and R.P.'s research was partially supported by the

CC	R_1	R_2	$\lvert A_6\rvert$
$++++++$			
$2.417991007837614 \cdot 10^{-17} - i\ 4.793031572579084 \cdot 10^{-17}$			
$-$	$-$	$-$	0.529806483643855
$-$	$-$	$-$	0.529806483661295
$4.105695207224680 \cdot 10^{-16}$	-0.1382337836650667	$-9.500309796373058 \cdot 10^{-2}$	0.529806483661327
$+i\ 1.504282270415678 \cdot 10^{-15}$	$+i\ 0.360080242802749$	$+i\ 0.1156249885933891$	
$-++++++$			
$9.755813312628327, \cdot 10^{-19} + i\ 1.353208509225273 \cdot 10^{-16}$			
$-$	$-$	$-$	3.25996704351899
$-$	$-$	$-$	3.25996705427236
$3.812889817765093 \cdot 10^{-10}$	1.762222300120013	$-3.777721263438941 \cdot 10^{-2}$	3.25996705427262
$+i\ 1.011089409856760 \cdot 10^{-9}$	$+i\ 2.633781480837803$	$+i\ 0.1327460047079652$	
$--++++$			
$-2.806856204696471 - i\ 28.35268397049988$			
$-$	$-$	$-$	1373.74753500854
$-$	$-$	$-$	1373.74753500828
33436785.84436276	-33438045.33273086	6.674685589922374	1373.74753500852
$-i\ 14771512.10073091$	$+i\ 14772021.20888190$	$+i\ 61.85407887654488$	
$-+-+-+$			
$3.131859164936308 - i\ 0.2073463331363808$			
$-$	$-$	$-$	151.043950328960
$-$	$-$	$-$	151.043950337947
-370592.0271294174	370518.3987124019	-6.563948999154568	151.043950337955
$+i\ 28580469.70894824$	$-i\ 28580599.25896605$	$+i\ 0.9730930522347396$	
$+-+-+-$			
$3.131859164936308 + i\ 0.2073463331363808$			
$-$	$-$	$-$	153.780101529836
$-$	$-$	$-$	153.780101415986
-370533.5799977572	370518.3987124019	-6.563948999154568	153.780101615242
$-i\ 28580750.73535662$	$+i\ 28580599.25896605$	$-i\ 0.9730930522347396$	

Table 1: Results for the finite part of the 1-loop virtual amplitudes for some helicity configurations for the case of six external gluons for the phase space point given in the text. The first row for each helicity configuration is the tree-order result. The second (unitarity) and the third (semi-numerical) rows are the results for $|A_6|$ taken from [23]. The fourth is our result for the cut-constructible, CC (with renormalization scale $\mu = \sqrt{s}$), R_1 and R_2 terms in the HV scheme as well as for the $|A_6|$ in FDH scheme, to facilitate comparisons. The relation of HV scheme result to the FDH scheme result is given in [23].

RTN European Programme MRTN-CT-2006-035505 (HEPTOOLS, Tools and Precision Calculations for Physics Discoveries at Colliders). The research of R.P., M.V.G. and P.D. was also supported by the MEC project FPA2008-02984.

Appendices

A. The needed integrals

In this appendix, we collect the integrals needed to perform our calculation of R_2. A non vanishing contribution is generated only by integrals with zero or higher superficial degree of divergence. They fall in two classes, namely integrals involving even powers of $\tilde{q}$ (odd powers do no contribute due to Lorentz invariance) and Pole Parts (P.P.) of ultraviolet divergent integrals. This second class is relevant when using regularization schemes (such

as the HV one) where the ϵ dependence in the numerator is kept. In the following, we further classify the integrals according to the number of denominators $\bar{D}_i = (\bar{q}+p_i)^2 - m_i^2$. The results for the Pole Parts have been checked against ref. [2].

2-point integrals:

$$\begin{aligned}
\int d^n\bar{q}\frac{\tilde{q}^2}{\bar{D}_i\bar{D}_j} &= -\frac{i\pi^2}{2}\left[m_i^2+m_j^2-\frac{(p_i-p_j)^2}{3}\right]+O(\epsilon)\,,\\
P.P.\left(\int d^n\bar{q}\frac{1}{\bar{D}_i\bar{D}_j}\right) &= -2\frac{i\pi^2}{\epsilon}\,,\\
P.P.\left(\int d^n\bar{q}\frac{q_\mu}{\bar{D}_i\bar{D}_j}\right) &= \frac{i\pi^2}{\epsilon}(p_i+p_j)_\mu\,,\\
P.P.\left(\int d^n\bar{q}\frac{q_\mu q_\nu}{\bar{D}_i\bar{D}_j}\right) &= \frac{i\pi^2}{3\epsilon}\Big\{\frac{(p_i-p_j)^2-3m_i^2-3m_j^2}{2}g_{\mu\nu}-2\,p_{i\mu}p_{i\nu}-2\,p_{j\mu}p_{j\nu}\\
&\quad -p_{i\mu}p_{j\nu}-p_{j\mu}p_{i\nu}\Big\}\,.
\end{aligned}\tag{A.1}$$

3-point integrals:

$$\begin{aligned}
\int d^n\bar{q}\frac{\tilde{q}^2}{\bar{D}_i\bar{D}_j\bar{D}_k} &= -\frac{i\pi^2}{2}+O(\epsilon)\,,\\
\int d^n\bar{q}\frac{\tilde{q}^2 q_\mu}{\bar{D}_i\bar{D}_j\bar{D}_k} &= \frac{i\pi^2}{6}(p_{ijk})_\mu+O(\epsilon)\,,\\
P.P.\left(\int d^n\bar{q}\frac{q_\mu q_\nu}{\bar{D}_i\bar{D}_j\bar{D}_k}\right) &= -\frac{i\pi^2}{2\epsilon}g_{\mu\nu}\,,\\
P.P.\left(\int d^n\bar{q}\frac{q_\mu q_\nu q_\rho}{\bar{D}_i\bar{D}_j\bar{D}_k}\right) &= \frac{i\pi^2}{6\epsilon}\Big[g_{\mu\nu}(p_{ijk})_\rho+g_{\nu\rho}(p_{ijk})_\mu+g_{\mu\rho}(p_{ijk})_\nu\Big]\,,
\end{aligned}\tag{A.2}$$

with $p_{ijk} = p_i + p_j + p_k$.

4-point integrals:

$$\begin{aligned}
\int d^n\bar{q}\frac{\tilde{q}^4}{\bar{D}_i\bar{D}_j\bar{D}_k\bar{D}_l} &= -\frac{i\pi^2}{6}+O(\epsilon)\,,\\
\int d^n\bar{q}\frac{\tilde{q}^2 q_\mu q_\nu}{\bar{D}_i\bar{D}_j\bar{D}_k\bar{D}_l} &= -\frac{i\pi^2}{12}g_{\mu\nu}+O(\epsilon)\,,\\
\int d^n\bar{q}\frac{\tilde{q}^2 q^2}{\bar{D}_i\bar{D}_j\bar{D}_k\bar{D}_l} &= -\frac{i\pi^2}{3}+O(\epsilon)\,,\\
P.P.\left(\int d^n\bar{q}\frac{q_\mu q_\nu q_\rho q_\sigma}{\bar{D}_i\bar{D}_j\bar{D}_k\bar{D}_l}\right) &= -\frac{i\pi^2}{12\epsilon}\Big(g_{\mu\nu}g_{\rho\sigma}+g_{\mu\rho}g_{\nu\sigma}+g_{\mu\sigma}g_{\nu\rho}\Big)\,.
\end{aligned}\tag{A.3}$$

B. QCD Feyman Rules and diagrams

In this appendix, we present the Feynman rules and the diagrams used in the calculation. In fig. 4 we list QCD propagators and vertices as well as our parametrization of the Vqq

and Sqq couplings. Ghosts are drawn with dashed arrows, vectors with wavy lines and scalars with dotted lines; Greek letters denote Lorentz indices; $k, l = 1, 2, 3$ are the three colors of the quarks while all remaining color indices range from 1 to 8; f^{abc} is the QCD $SU(N_{col})$ structure constant and t^a ($a = 1, \cdots, 8$) are the color matrices in the fundamental representation; m_q is the quark mass and $V_{\mu_1\mu_2\mu_3}(p_1, p_2, p_3)$ is given by

$$V_{\mu_1\mu_2\mu_3}(p_1, p_2, p_3) = g_{\mu_1\mu_2}(p_2 - p_1)_{\mu_3} + g_{\mu_2\mu_3}(p_3 - p_2)_{\mu_1} + g_{\mu_3\mu_1}(p_1 - p_3)_{\mu_2} \,. \qquad \text{(B.1)}$$

Finally, in fig. 5 and 6, we draw the pure QCD graphs and the mixed QCD diagrams which give a non vanishing contribution to R_2. As explained in section 2, diagrams involving QCD FP ghosts do not to contribute to R_2 and are not included.

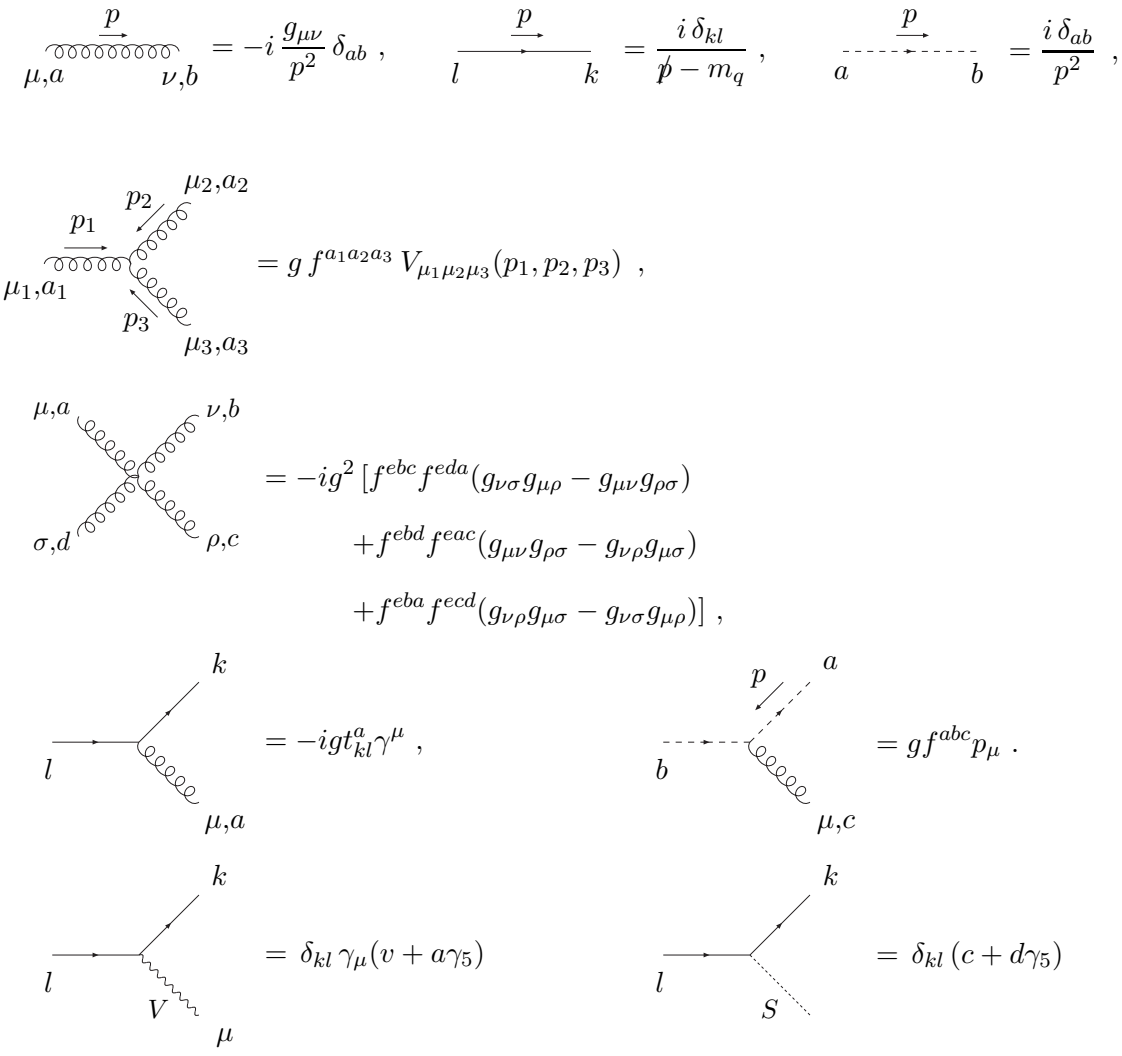

Figure 4: *Feynman rules used for the computation. The last two vertices parametrize a generic coupling of a (pseudo)-vector V and of a (pseudo)-scalar S with a quark line, respectively.*

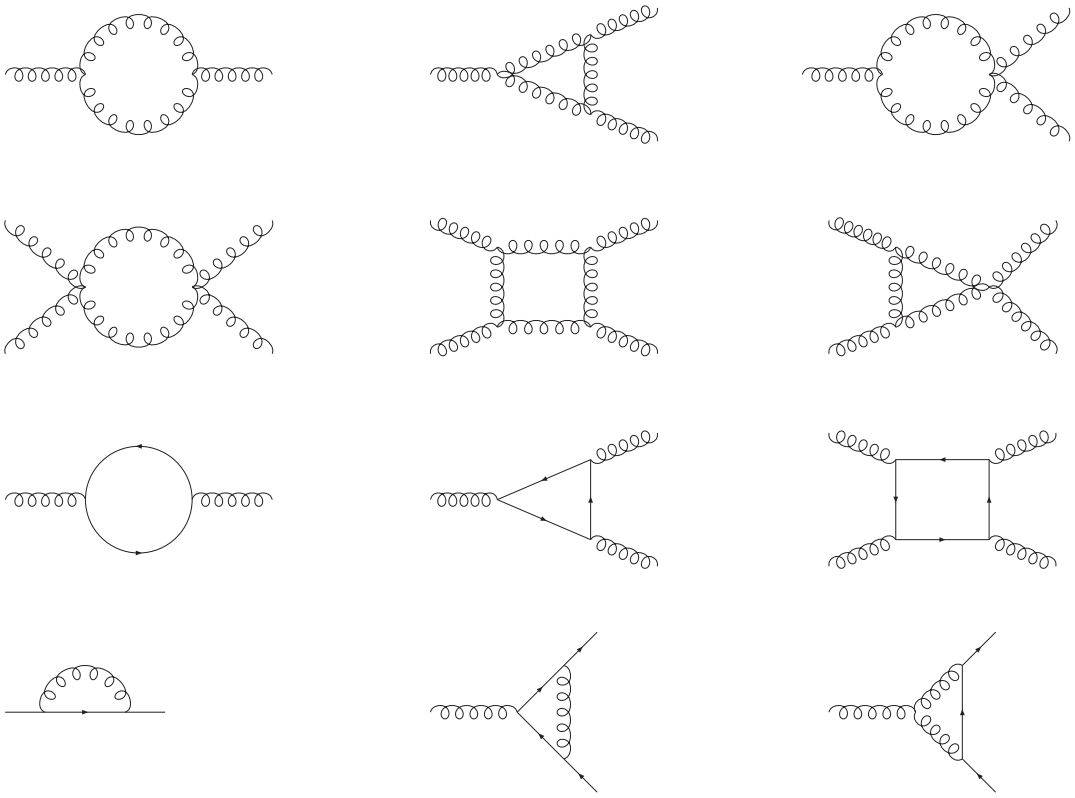

Figure 5: *Pure QCD diagrams used for the calculation.*

C. Effective vertices in the color connection language

In this appendix, we write down the Feynman rules for the QCD effective vertices in the color connection language. Such rules are obtained by contracting any gluon index a_i, appearing in the vertices of figs. 2 and 3 , by a color matrix $t^{a_i}_{k_i l_i}$. Any gluonic color index a_i is therefore projected out in terms of two quark like color and anti-color indices k_i and l_i. By then summing over gluon indices with the rule

$$t^a_{kl} t^a_{ij} = \frac{1}{2}\left[\delta_{kj}\delta_{il} - \frac{1}{N_{col}}\delta_{kl}\delta_{ij}\right] , \tag{C.1}$$

the color part of the effective vertices can be entirely written down in terms of δ's, which correspond to color connections. Graphically, a color connection can be represented with a solid line, in such a way that two solid lines stand for a gluon, while one single solid line symbolize a quark. Finally, different color lines can be connected by the exchange of a scalar colorless gluon, represented by a dashed line. In such a language, the pure QCD effective vertices of fig. 2 can be written as in figs. 7 and 8. Analogously, the last five mixed QCD vertices of fig. 3 give the results reported in figs. 9-11.

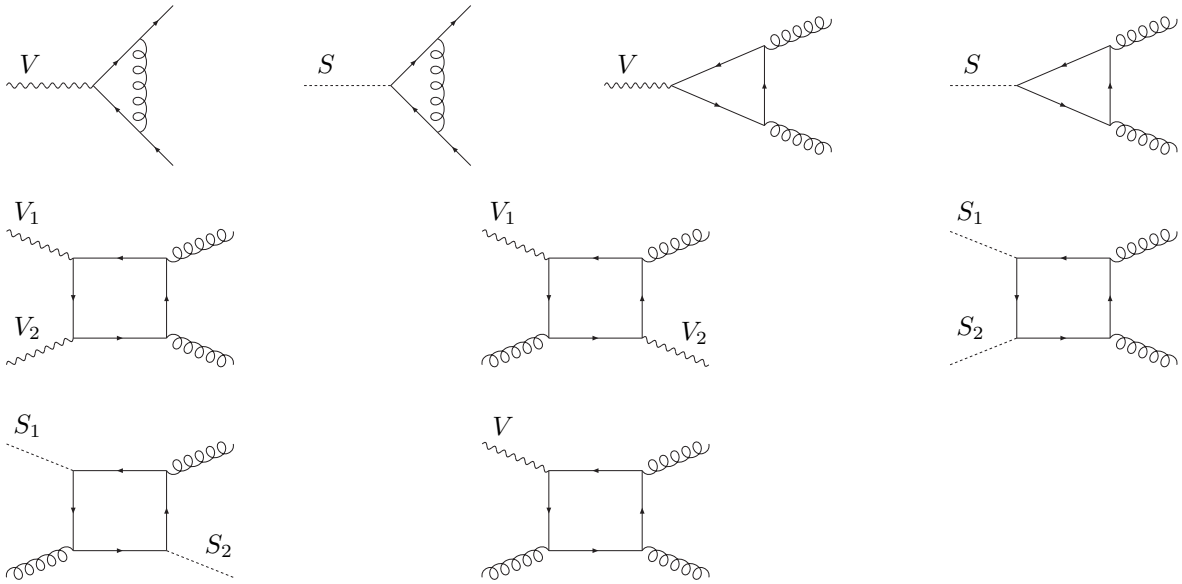

Figure 6: *Mixed QCD diagrams contributing to* R_2.

References

[1] G. Passarino and M. J. G. Veltman, Nucl. Phys. B **160** (1979) 151.

[2] A. Denner, Fortsch. Phys. **41** (1993) 307 [arXiv:0709.1075 [hep-ph]].

[3] J. Kublbeck, M. Bohm and A. Denner, Comput. Phys. Commun. **60** (1990) 165;
R. Mertig, M. Bohm and A. Denner, Comput. Phys. Commun. **64** (1991) 345;
A. Denner and S. Dittmaier, Nucl. Phys. B **658** (2003) 175 [arXiv:hep-ph/0212259];
A. Ferroglia, M. Passera, G. Passarino and S. Uccirati, Nucl. Phys. B **650** (2003) 162 [arXiv:hep-ph/0209219];
T. Diakonidis, J. Fleischer, J. Gluza, K. Kajda, T. Riemann and J. B. Tausk, arXiv:0812.2134 [hep-ph].

[4] T. Binoth, J. P. Guillet, G. Heinrich, E. Pilon and C. Schubert, JHEP **0510**, 015 (2005) [arXiv:hep-ph/0504267];
T. Binoth, J. P. Guillet, G. Heinrich, E. Pilon and T. Reiter, arXiv:0810.0992 [hep-ph];
T. Binoth *et al.*, arXiv:0807.0605 [hep-ph].

[5] A. Denner, S. Dittmaier, M. Roth and D. Wackeroth, Phys. Lett. B **475** (2000) 127 [arXiv:hep-ph/9912261];
G. Montagna, F. Piccinini, O. Nicrosini, G. Passarino and R. Pittau, Comput. Phys. Commun. **76** (1993) 328;
D. Y. Bardin, P. Christova, M. Jack, L. Kalinovskaya, A. Olchevski, S. Riemann and T. Riemann, Comput. Phys. Commun. **133** (2001) 229 [arXiv:hep-ph/9908433];
T. Hahn and M. Perez-Victoria, Comput. Phys. Commun. **118** (1999) 153 [arXiv:hep-ph/9807565].

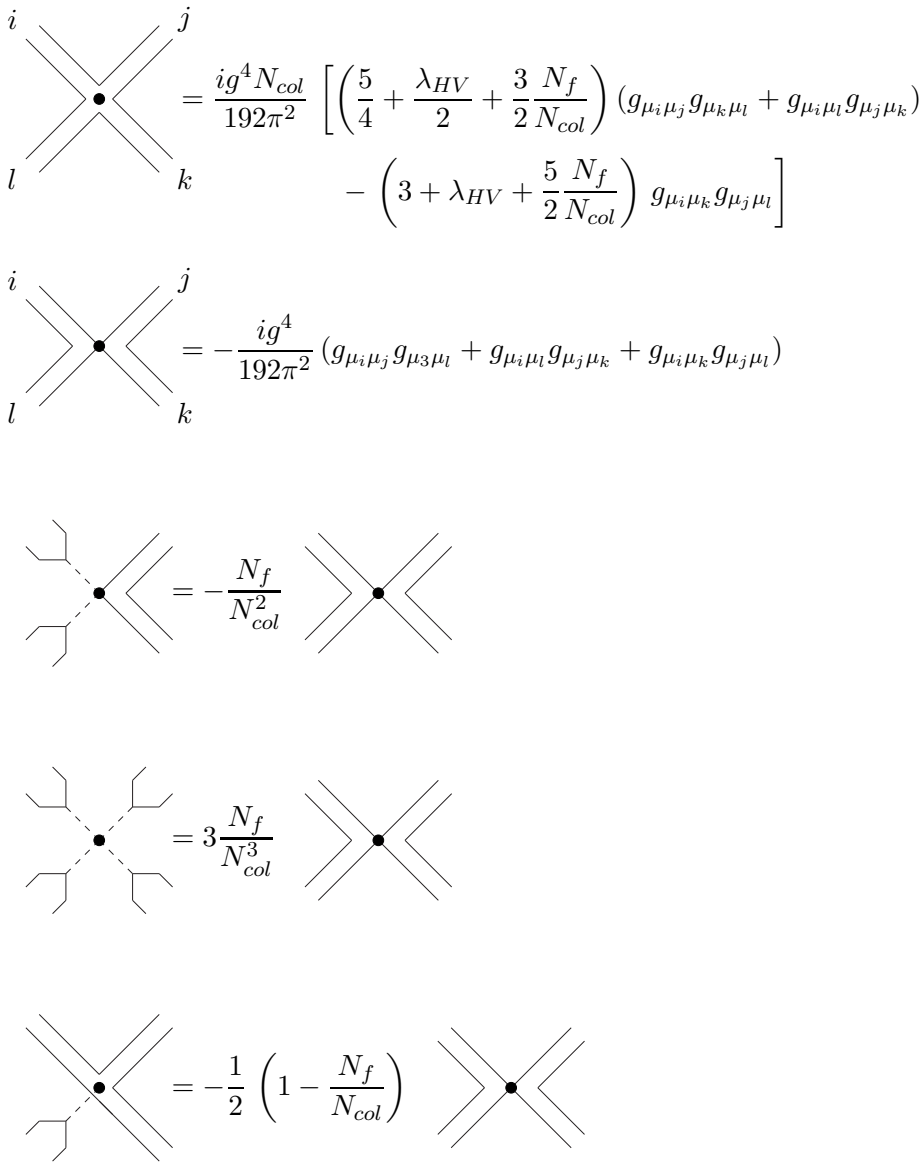

Figure 7: *Effective 4-gluon vertices contributing to* R_2 *in pure QCD in the color connection language.* N_f *is the number of fermions running in the quark loop.*

[6] Z. Bern, L. J. Dixon, D. C. Dunbar and D. A. Kosower, Nucl. Phys. B **435** (1995) 59 [arXiv:hep-ph/9409265] and Nucl. Phys. B **425**, 217 (1994). See also Z. Bern, L. J. Dixon and D. A. Kosower, Annals Phys. **322** (2007) 1587 [arXiv:0704.2798 [hep-ph]].

[7] Z. Bern, L. J. Dixon and D. A. Kosower, Phys. Rev. Lett. **70** (1993) 2677 [arXiv:hep-ph/9302280];
Z. Bern, L. J. Dixon and D. A. Kosower, Nucl. Phys. B **513** (1998) 3 [arXiv:hep-ph/9708239];
Z. Bern, L. J. Dixon and D. A. Kosower, Nucl. Phys. B **437** (1995) 259 [arXiv:hep-ph/9409393];

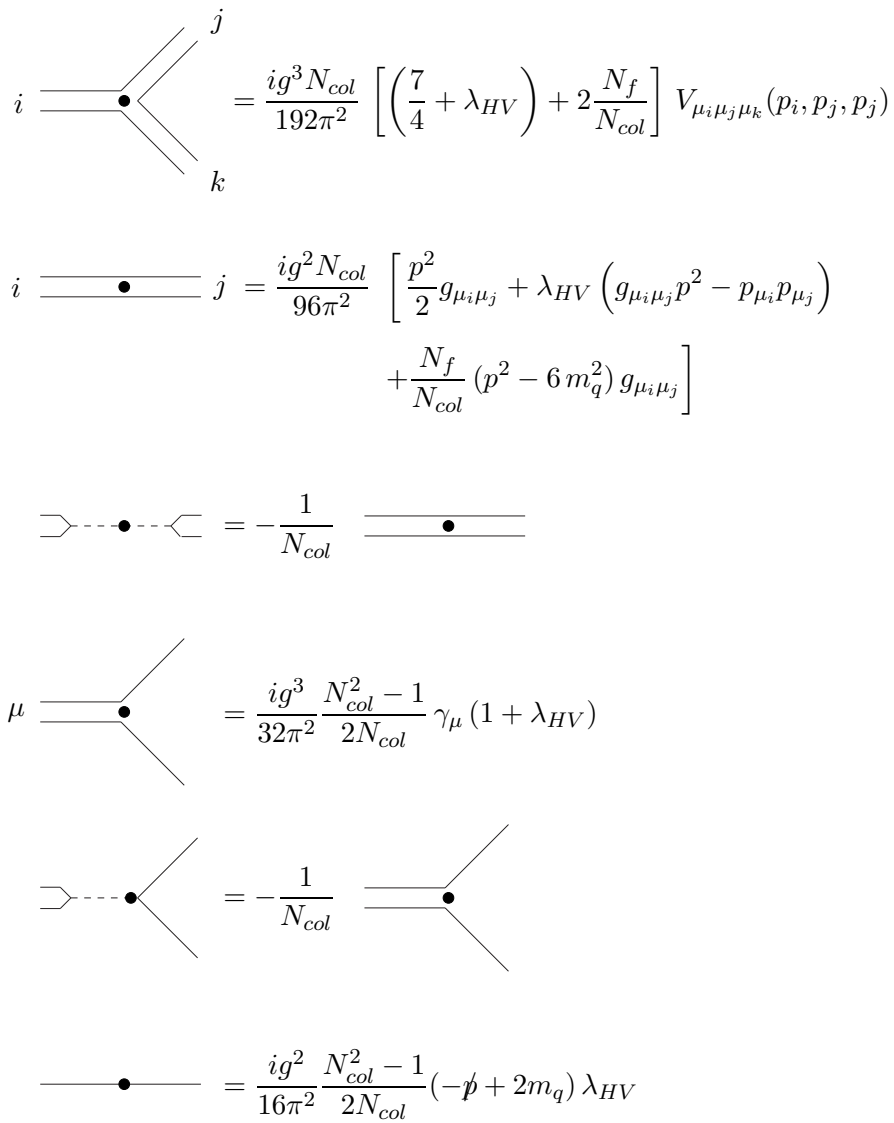

Figure 8: *Effective 3- and 2- point vertices contributing to* R_2 *in pure QCD in the color connection language. All momenta are incoming. The first three diagrams represent the ggg and gg vertices; the last three qqg and qq.* N_f *is the number of fermions running in the quark loop.*

C. F. Berger, Z. Bern, L. J. Dixon, D. Forde and D. A. Kosower, Phys. Rev. D **74** (2006) 036009 [arXiv:hep-ph/0604195].

[8] R. Britto, F. Cachazo and B. Feng, Nucl. Phys. B **725**, 275 (2005).

[9] G. Ossola, C. G. Papadopoulos and R. Pittau, Nucl. Phys. B **763** (2007) 147 [arXiv:hep-ph/0609007].

[10] G. Ossola, C. G. Papadopoulos and R. Pittau, JHEP **0803** (2008) 042 [arXiv:0711.3596 [hep-ph]]. See also P. Mastrolia, G. Ossola, C. G. Papadopoulos and R. Pittau, JHEP **0806** (2008) 030 [arXiv:0803.3964 [hep-ph]].

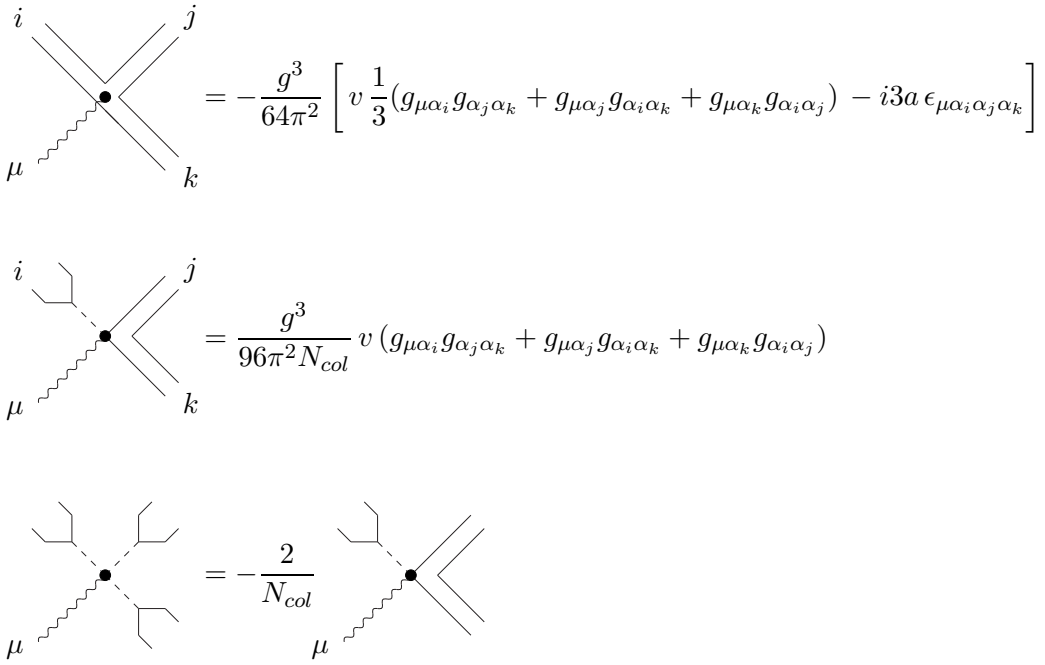

Figure 9: *Effective Vggg vertex contributing to* R_2 *in mixed QCD in the color connection language (contribution of one quark loop).*

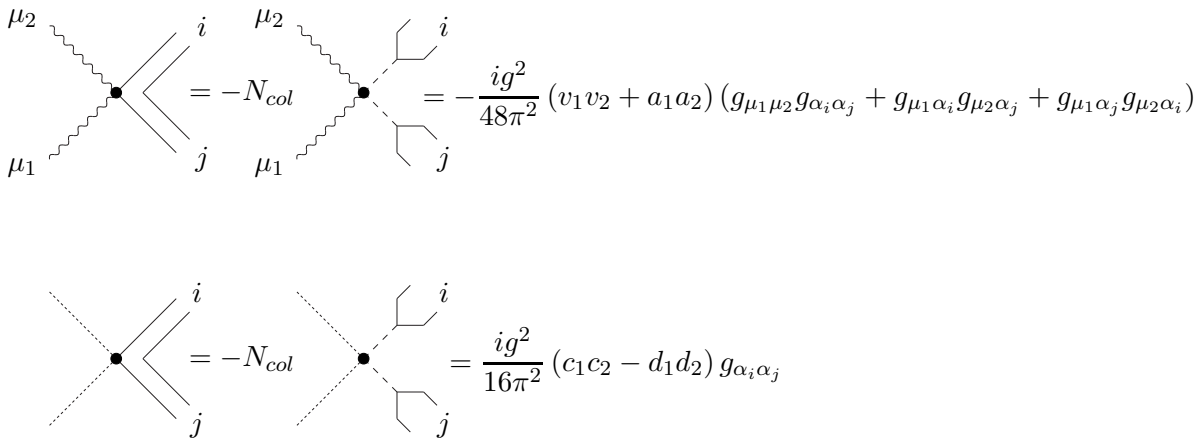

Figure 10: *Effective VVgg and SSgg vertices contributing to* R_2 *in mixed QCD in the color connection language. In the case of neutral external vectors or scalars, the formulae should be read as the contribution given by one quark loop. In the case of charged external particles, they refer instead to the contribution of one quark family.*

[11] F. del Aguila and R. Pittau, JHEP **0407** (2004) 017 [arXiv:hep-ph/0404120] and R. Pittau, arXiv:hep-ph/0406105.

[12] R. K. Ellis, W. T. Giele and Z. Kunszt, JHEP **0803** (2008) 003 [arXiv:0708.2398 [hep-ph]].

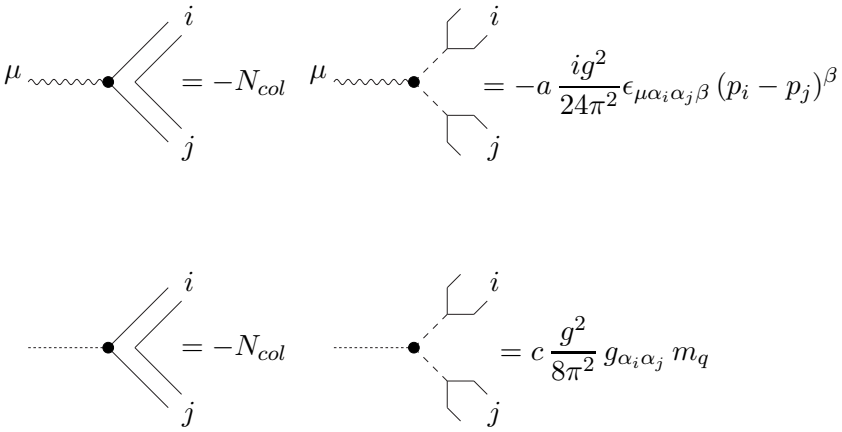

Figure 11: *Effective Vgg and Sgg vertices contributing to* R_2 *in mixed QCD in the color connection language (contribution of one quark loop). All momenta are incoming.*

[13] C. F. Berger *et al.*, Phys. Rev. D **78**, 036003 (2008) [arXiv:0803.4180 [hep-ph]]; W. B. Kilgore, arXiv:0711.5015 [hep-ph].

[14] W. T. Giele, Z. Kunszt and K. Melnikov, JHEP **0804** (2008) 049 [arXiv:0801.2237 [hep-ph]].

[15] A. Lazopoulos, arXiv:0812.2998 [hep-ph].

[16] T. Binoth, J. P. Guillet and G. Heinrich, JHEP **0702** (2007) 013 [arXiv:hep-ph/0609054]; A. Bredenstein, A. Denner, S. Dittmaier and S. Pozzorini, the JHEP **0808** (2008) 108 [arXiv:0807.1248 [hep-ph]].

[17] Z. G. Xiao, G. Yang and C. J. Zhu, Nucl. Phys. B **758** (2006) 1 [arXiv:hep-ph/0607015]; X. Su, Z. G. Xiao, G. Yang and C. J. Zhu, Nucl. Phys. B **758** (2006) 35 [arXiv:hep-ph/0607016].

[18] Z. Bern and A. G. Morgan, Nucl. Phys. B **467**, 479 (1996) [arXiv:hep-ph/9511336]; Z. Bern, L. J. Dixon, D. C. Dunbar and D. A. Kosower, Phys. Lett. B **394**, 105 (1997) [arXiv:hep-th/9611127];
C. Anastasiou, R. Britto, B. Feng, Z. Kunszt and P. Mastrolia, Phys. Lett. B **645**, 213 (2007) [arXiv:hep-ph/0609191];
R. Britto and B. Feng, JHEP **0802**, 095 (2008) [arXiv:0711.4284 [hep-ph]];
R. Britto, B. Feng and P. Mastrolia, Phys. Rev. D **78**, 025031 (2008) [arXiv:0803.1989 [hep-ph]];
R. K. Ellis, W. T. Giele, Z. Kunszt and K. Melnikov, arXiv:0806.3467 [hep-ph].

[19] Z. Bern, L. J. Dixon and D. A. Kosower, Phys. Rev. D **71**, 105013 (2005) [arXiv:hep-th/0501240], Phys. Rev. D **72**, 125003 (2005) [arXiv:hep-ph/0505055] and Phys. Rev. D **73**, 065013 (2006) [arXiv:hep-ph/0507005];
C. F. Berger, Z. Bern, L. J. Dixon, D. Forde and D. A. Kosower, Phys. Rev. D **74**, 036009 (2006) [arXiv:hep-ph/0604195].

[20] G. Ossola, C. G. Papadopoulos and R. Pittau, JHEP **0805** (2008) 004 [arXiv:0802.1876 [hep-ph]] and JHEP **0707** (2007) 085 [arXiv:0704.1271 [hep-ph]].

[21] A. van Hameren, C. G. Papadopoulos and R. Pittau, arXiv:0903.4665 [hep-ph].

[22] A. Kanaki and C. G. Papadopoulos, Comput. Phys. Commun. **132** (2000) 306 [arXiv:hep-ph/0002082];
A. Kanaki and C. G. Papadopoulos, arXiv:hep-ph/0012004.
A. Cafarella, C. G. Papadopoulos and M. Worek, arXiv:0710.2427 [hep-ph].

[23] W. T. Giele and G. Zanderighi, arXiv:0805.2152 [hep-ph].

[24] Z. Bern *et al.* [NLO Multileg Working Group], arXiv:0803.0494 [hep-ph].